

PARAMETRIC DECAY IN THE EDGE PLASMA OF
ASDEX DURING FAST WAVE HEATING IN THE
ION CYCLOTRON FREQUENCY RANGE

R. Van Nieuwenhove and G. Van Oost¹

J.-M. Noterdaeme, M. Brambilla, J. Gernhardt²

M. Porkolab³

IPP III/129

January 1988



MAX-PLANCK-INSTITUT FÜR PLASMAPHYSIK

8046 GARCHING BEI MÜNCHEN

MAX-PLANCK-INSTITUT FÜR PLASMAPHYSIK

GARCHING BEI MÜNCHEN

PARAMETRIC DECAY IN THE EDGE PLASMA OF
ASDEX DURING FAST WAVE HEATING IN THE
ION CYCLOTRON FREQUENCY RANGE

R. Van Nieuwenhove and G. Van Oost¹

J.-M. Noterdaeme, M. Brambilla, J. Gernhardt²

M. Porkolab³

IPP III/129

January 1988

- 1) Laboratoire de Physique des Plasmas - Laboratorium voor
Plasmafysica, Association "Euratom-Etat belge" -
Associatie "Euratom-Belgische Staat" - Ecole Royale
Militaire - B 1040 Brussels - Koninklijke Militaire School
- 2) Max-Planck-Institut für Plasmaphysik, Euratom Association
D-8046 Garching, Federal Republic of Germany
- 3) Department of Physics and Plasma Fusion Center
Massachusetts Institute of Technology
Cambridge, Massachusetts 02139

*Die nachstehende Arbeit wurde im Rahmen des Vertrages zwischen dem
Max-Planck-Institut für Plasmaphysik und der Europäischen Atomgemeinschaft über die
Zusammenarbeit auf dem Gebiete der Plasmaphysik durchgeführt.*

**PARAMETRIC DECAY IN THE EDGE PLASMA OF
ASDEX DURING FAST WAVE HEATING IN THE ION CYCLOTRON
FREQUENCY RANGE**

R. Van Nieuwenhove and G. Van Oost

Laboratoire de Physique des Plasmas - Laboratorium voor Plasmafysica

Association "Euratom-Etat belge" - Associatie "Euratom-Belgische Staat"

Ecole Royale Militaire - B 1040 Brussels - Koninklijke Militaire School

J.-M. Noterdaeme, M. Brambilla, J. Gernhardt

Max-Planck-Institut für Plasmaphysik, Euratom Association

D-8046 Garching, Federal Republic of Germany

M. Porkolab

Department of Physics and Plasma Fusion Center

Massachusetts Institute of Technology

Cambridge, Massachusetts 02139

Abstract.

Two types of parametric decay instabilities were observed in the scrape-off layer of ASDEX during hydrogen second harmonic heating, in the single- as well as in a two-ion-species plasma. The first type was identified as decay into an ion Bernstein wave and an ion cyclotron quasimode, and the second as decay into an ion Bernstein wave and a low frequency electron quasimode. The parametric decay processes are due to the high electric fields near the fast wave antennas. Theoretical growth rate calculations predict a threshold electric field which is in reasonable agreement with the values estimated from a full-wave code, modelling the relevant experiments. These parametric decay processes, as well as the harmonics of the generator frequency also seen in the scrape-off layer, provide a mechanism that might contribute to the observed direct energy deposition in the edge plasma and to ICRF-induced impurity production.

1. Introduction.

The study of the effects of ICRF on the plasma edge parameters is becoming increasingly important. Indeed, there is growing evidence for a direct link between the bulk plasma properties and the edge plasma parameters, which are influenced by the RF fields. Furthermore the study of the interactions between the RF fields and the edge plasma may provide clues to the physical mechanisms responsible for ICRF-induced side effects [see e.g. 1-9] such as enhanced recycling, creation of fast ions, impurity production, etc. A thorough understanding of these phenomena may be the way to improve antenna design as well as the operating scenarios so as to minimize the impact on the plasma heating performance.

At the high power levels required for additional heating of tokamaks, various nonlinear phenomena, and in particular parametric decay processes near the plasma edge can occur. Under the influence of an externally applied high frequency electromagnetic field, various modes of the plasma may become coupled and driven unstable, especially near the ICRF antennas where RF electric fields of the order of 200 V/cm may exist for launched powers of the order of 1 MW. These parametric decay processes are important; they are a candidate to explain the observed direct energy deposition in the plasma edge which could lead to ICRF-induced impurity problems.

This letter reports on parametric decay instabilities, which were for the first time observed in the scrape-off layer of an ICRF-heated tokamak in a single- as well as in a two-ion-species plasma, and relates them to some theoretical predictions. Up to now, these processes have been observed to occur in the hydrogen second harmonic heating scheme, whilst in the minority heating scheme fewer measurements were available from which no conclusions can be drawn. Theoretical work indicates that two types of decay processes may be occurring in the present experiments: (1) decay into an ion Bernstein wave and an ion cyclotron quasimode (2) decay into an ion Bernstein wave and a low frequency electron quasimode. Both have been observed on ASDEX.

The plan of the letter is as follows: in Sect. 2 the experiments are described and experimental results are presented; in Sect. 3 theoretical considerations and a comparison with experimental data are given; finally in Sect. 4 the results are summarized and discussed.

2. Experimental Results.

Measurements were performed during ICRF heating of an ohmic plasma or of plasma preheated by NI($H^0 \rightarrow D^+, E_0 = 40 \text{ keV}$, $P_{NI} = 0.8 - 3.5 \text{ MW}$) in the divertor tokamak ASDEX. The ICRF heating schemes were hydrogen minority heating (D(H), 33.5 MHz, $n_H/n_e \simeq 5 \%$) and hydrogen second harmonic heating ($2\omega_{CH}$, 67 MHz) in pure hydrogen plasmas or hydrogen-deuterium mixtures ($n_H/(n_H + n_D) = 25 - 100 \%$). Up to $P_{IC} \simeq 2.6 \text{ MW}$ of RF power was launched by two low field side antennas [10- 12] .

Typical ohmic target plasma parameters were $R_p = 1.67 \text{ m}$, $a_p = 0.40 \text{ m}$ (Fig. 1b), $I_p = 380 \text{ kA}$, $B_0(\text{at } R_0 = 1.65 \text{ m}) \simeq 2.24 \text{ T}$, $P_{OH} = 450 \text{ kW}$, $\bar{n}_e = 2 - 6 \times 10^{13} \text{ cm}^{-3}$, $T_{eo} \simeq 650 \text{ eV}$, $T_{io} \simeq 550 \text{ eV}$. With NI preheating the target plasma temperatures rised to $T_{eo} \simeq 1.2 \text{ keV}$, $T_{io} \simeq 2 \text{ keV}$. The ion cyclotron resonance layer was positioned between $r = -23 \text{ cm}$ and $r = +38 \text{ cm}$ with respect to the plasma centre by scanning B_0 .

Figure 1(a) presents a top view of ASDEX, showing the locations of the ICRF fast wave antennas and the electrical probe with which parametric decay wave spectra were observed. Two loop antennas are installed at the low magnetic field side, at opposite toroidal locations; they are fed at both ends and short-circuited in the midplane. The electrical length of one loop (half antenna) is about $\lambda / 4$ for the hydrogen second harmonic frequency range (67 MHz). Carbon guard limiters on both sides protect the antennas. The poloidal cross section of ASDEX in Fig. 1(b) shows the radial location of the antenna, separatrix, wall components, and RF probe. The 20 cm long, horizontally oriented cylindrical electric probe monitors the RF electric fields in the scrape-off layer (SOL) of ASDEX. It is positioned about 60 cm away from one ICRF antenna in the toroidal direction, 4 cm behind the antenna protection limiter, and 20 cm below the equatorial plane. This probe configuration does not provide spatial resolution. Parametric decay phenomena were observed both when the antenna close to the probe and when the opposite antenna was excited.

A frequency spectrum of the parametric decay instabilities observed in a mixture of hydrogen and deuterium with $2\omega_{CH}$ heating is shown in Fig. 2(a). The spectrum reveals the two types of parametric decay corresponding to the sidebands 2_e and 2_H (ion Bernstein waves, IBW) and the low frequency decay waves 1_e (electron quasimode, here not observable due to the zero frequency peak of the spectrum analyzer) and 1_H (hydrogen ion cyclotron quasimode, QM, excited near the ion cyclotron frequency in the SOL). Throughout the text, the indices 0,1,2 and 3 refer to pump, low frequency decay mode, lower sideband wave, and upper sideband wave, respectively. The upper

sidebands are not always present. Due to the uncalibrated probe configuration, no conclusions can be drawn from the absolute amplitude of the different modes. The spectrum of Fig. 2(b) was also observed for a mixture of hydrogen and deuterium with $2\omega_{CH}$ heating. This spectrum again reveals the presence of both types of decay instabilities, but this time the deuterium ion cyclotron QM(1_D) as well as the hydrogen ion cyclotron QM (1_H) appear, together with the corresponding IBW's 2_D and 2_H . In the case of a pure hydrogen plasma, a spectrum similar to the one in Fig. 2(a) was observed, with only the hydrogen ion cyclotron QM present, besides the electron QM.

Similar decay spectra were also observed during preliminary measurements with a pickup antenna located at the high field side of ASDEX. The observed decay wave frequencies for several values of B_0 are plotted in Fig. 3, and compared with the values expected from the selection rule $\omega_0 = \omega_1 + \omega_2$, with $\omega_1 \simeq \omega_{CD}$, ω_{CH} in the SOL ($R = 2.08$ m).

The electrical probe data also reveals the presence of harmonics of the RF generator frequency [13], sometimes accompanied by parametric decay. The generation of these harmonics could be due to a nonlinear sheath effect at the antenna, similar to that observed when using an electrostatic type of antenna [14,15]. Under some conditions splitting of decay frequency peaks was observed.

3. Theoretical Considerations.

Theoretical ion Bernstein wave dispersion curves were calculated for parameters representative of the ASDEX edge plasma. Examples for a pure hydrogen plasma and for a mixture of hydrogen and deuterium are plotted in Fig. 4 (a) and 4(b), respectively. A typical decay pattern for decay into an ion QM and an IBW is also indicated.

Calculations of the electric field components in the neighbourhood of an ICRF antenna were performed using a full-wave one-dimensional code [16, see also 17]. For the case of a pure hydrogen plasma, a launched RF power of 1 MW, and $B_0 = 2.05$ T, an electric field of about 200 V/cm is found (E_x and E_y are comparable). For a mixture of hydrogen and deuterium, the electric field was calculated for several values of the magnetic field. It is found to vary between 120 V/cm at $B_0 = 1.92$ T and 400 V/cm at $B_0 = 2.73$ T. It is presently unclear why, with a continuous variation of the electric field, the parametric decay is only found to occur for specific values of B_T (see Fig.3). It may be a consequence of threshold effects which are under study [18].

In the following the parametric growth rates and thresholds will be derived in the heating regimes $\omega_0 \sim \omega_{CH}(0) = 2\omega_{CD}(0)$ and $\omega_0 \sim 2\omega_{CH}(0)$ where $\omega_{CH}(0)$, $\omega_{CD}(0)$ refer to the proton and deuteron ion cyclotron frequency at the centre of the plasma column, respectively. In the edge region the second harmonic hydrogen heating scenario is most susceptible to parametric instabilities for the electric fields and plasma parameters of interest. In the ASDEX experiments, the fixed pump wave frequency ($\omega_0 = 2\pi \times 67 \text{ MHz}$) corresponds for the different values of the magnetic field to $\omega_0/\omega_{CH} = 2.05$ to 2.7 , where ω_{CH} is the hydrogen cyclotron frequency in the SOL ($R = 2.08 \text{ m}$). In many experiments a substantial amount of deuterium may also be present due to hydrogen beam injection into the deuterium majority plasma (or vice versa). Therefore the presence of a second ion species, and hence the relative RF drift motion of the two species induced by the pump due to their different masses, must also be considered for it may substantially alter the thresholds and/or the decay wave spectrum, as is observed in the ASDEX experiments.

Theoretical studies [19-23] indicate that for the present situation the dominant decay processes involve nonresonant low frequency quasimodes ¹ driven by electrons and with a parallel phase velocity such that $\omega_1 \simeq k_{||1} V_{te}$, where V_{te} is the electron thermal velocity. Two types of QM can occur: (1) QM's that are also resonant with ions through ion cyclotron resonance interaction ($|\omega_1 - \omega_{ci}|/k_{||1} V_{ti} \leq 1$) , so that $\omega_1 \simeq \omega_{CD}, \omega_{CH}$; (2) low frequency QM's with $\omega_1 \ll \omega_{CD}, \omega_{CH}$; $\omega_1 \leq k_{||1} V_{te}$. In both cases the sidebands involved are IBW's. In general, both types of decay modes may be present, however, the ion cyclotron QM's are more easily excited in a two-ion-species plasma. In a single-ion-species second harmonic heating or in a minority heating experiment, the threshold conditions are only marginally satisfied. Decay into the low frequency electron QM is relatively easy to obtain.

A summary of theoretical predictions will now be presented; the details will be given in a separate publication [18].

¹ These quasimodes do not obey a linear dispersion relation of the plasma and exist only in the presence of the pump field.

(a) Decay into a ion cyclotron QM and an IBW.

The growth rate γ_0 of the decay instabilities in a two-ion-species plasma, with $\omega_0 > 2\omega_{cj}$, is given by the following approximate expression (where only the dominant terms have been kept).

$$\frac{\gamma_{0j}}{\omega_2} = -\frac{\gamma_{2j}}{\omega_2} + \frac{1}{8} \frac{|\bar{V}_0 \times k_\perp|^2}{\omega_0^2} \frac{\sqrt{\pi} \zeta_e \exp(-\zeta_e^2)}{\left(\frac{n_H}{n_e}\right) P_H \left[1 + \frac{n_D}{n_H} \frac{P_D}{P_H}\right]} \quad [1]$$

The first term at the right-hand side corresponds to the losses inherent to the decay instability (γ_2 is the linear damping rate of the IBW at the sideband, $\omega_2 = \omega_0 - \omega_{cj}$); the second term corresponds to the drive term of the instability. The threshold value of E_0 (intervening in \bar{V}_0), above which the instability starts, is obtained by putting $\gamma_{0j} = 0$ in Eq(1). In Eq(1) $j = H, D$, $|\bar{V}_0 \times k_\perp| = V_{0\perp} k_\perp \sin \theta$, $V_0 = cE_{0\perp}/B$, and θ is the angle between $\bar{V}_{0\perp}$ and k_\perp ; $|k_\perp|$ is the perpendicular decay wave number of the instability ($\bar{k}_{\perp 0} = \bar{k}_{\perp 1} + \bar{k}_{\perp 2} \simeq 0$; the perpendicular pump wavenumber can be ignored in comparison with those of the decay waves). In the present situation $E_{0x} \simeq E_{0y}$ and $k_x \simeq k_y$, $\sin \theta \simeq 1$ for $\theta \simeq \pi/2$. In particular, the instability is driven by the electron $\bar{E} \times \bar{B}$ drift, although there may be a small contribution (of the order of 20 %) from the relative ion-ion drift. Furthermore, $\zeta_e = \omega/k_{\parallel} V_{te}$ with $V_{te}^2 = 2T_e/m_e$; n_H and n_D are the relative hydrogen and deuterium concentrations, respectively; finally,

$$P_j = \sum_{l=1}^{\infty} \frac{2l^2 \omega_{cj}^2 \Gamma_l(b_j) \omega_2^2}{(\omega_2^2 - l^2 \omega_{cj}^2)^2} = \frac{\omega_2 k^2 \lambda_{Dj}^2}{2} \frac{\partial \varepsilon}{\partial \omega_2} ; \quad \gamma_{2j} = \frac{\frac{v_{ei}}{\omega_2} \left(\frac{k_{\parallel 12}}{k_2}\right)^2 \frac{m_i}{m_e} \frac{\omega_{cj}^2}{\omega_2^2}}{\frac{2}{\omega_2} \frac{1}{b_j} P_j} \quad [2]$$

Here $\omega_2 = \omega_0 - \omega_1 \simeq \omega_0 - \omega_{cj}$; $\Gamma_l = I_l(b_j) e^{-b_j}$, $b_j = k_\perp^2 r_{cj}^2$, I_l is the modified Bessel function of the first kind, r_{cj} is the Larmor radius of the species j , λ_{Dj} is the Debye length of the species j , ε is the plasma dielectric constant for the sideband mode, and v_{ei} is the electron-ion collision frequency. The contribution of the upper sideband as well as the coupling to higher harmonics have been ignored in a first approximation. To minimize the threshold and maximize the growth rate of the decay instability, it has been assumed that $k_{\parallel 12}$ is small in order to reduce electron Landau damping at the sideband. In particular, in the ASDEX experiments, $k_{\parallel 12} = k_{\parallel 11} - k_{\parallel 10}$ (from the selection rule), with $k_{\parallel 10} \simeq 0.2 \text{ cm}^{-1}$, $k_{\parallel 11} \simeq 0.45 \text{ cm}^{-1}$, and hence $k_{\parallel 12} \simeq 0.25 \text{ cm}^{-1}$.

For the case of a pure hydrogen plasma with the same parameters, $\gamma_2 \approx 1 \times 10^4 \text{ s}^{-1}$, and electron Landau damping at the sideband is comparable to or smaller than γ_2 . Assuming that $E_{0x} \approx E_{0y} \approx 200 \text{ V/cm}$, (E_0 included in V_0) for $\omega_0 = 2.75 \omega_{CH}$, the growth rate is $\gamma_0 \approx 5 \times 10^5 \text{ s}^{-1}$ for $\sin \theta \approx 1$ and $\zeta_e \approx 0.7$. For the case of a mixture of hydrogen (30 %) and deuterium (70 %), Eq(1) was evaluated for $\omega_0/\omega_{CH} = 2.75$, $\omega_2/\omega_{CH} = 1.75$, $\omega_1/\omega_{CH} = 1$, and $\zeta_e = 0.7$. For $E_{0x} \approx E_{0y} \approx 200 \text{ V/cm}$, Eq(1) predicts a growth rate of $\gamma_0 \approx 1.8 \times 10^6 \text{ s}^{-1}$.

While the dissipative thresholds are easily exceeded, the relevant threshold is that imposed by convective losses. The decay waves may escape from the finite amplification region before they can grow to a sufficiently large amplitude. The radial extent of the amplification region for the ion cyclotron QM is given by $\Delta x = 2 L_B k_{||1} V_{ti}/\omega_{CH} \approx 7 \text{ cm}$ (L_B is the gradient scale length of B_T), and hence the amplification distance is $\Delta r \approx \Delta x / \sin(\theta/2) \approx \sqrt{2} \Delta x$, or approximately 10 cm. Therefore, the total convective growth exponent is $\gamma_0 \Delta r / V_g$, where $V_g \approx V_{ti}$ is the group velocity for $\omega_2/\omega_{CH} = 1.75$, $\omega_0/\omega_{CH} = 2.75$, $b_i \approx 0.5$. For $T_i \approx 25 \text{ eV}$, $V_{ti} \approx 5 \times 10^6 \text{ cm/s}$ in a hydrogen plasma. In a single-ion-species plasma for $E_{0x} \approx E_{0y} \approx 200 \text{ V/cm}$, $\gamma_0 \approx 5 \times 10^5 \text{ s}^{-1}$, so that $\gamma_0 \Delta r / V_g \approx 1$ for $\Delta r \approx 10 \text{ cm}$. In a mixture of hydrogen (30 %) and deuterium (70 %), with $V_g \approx 6 \times 10^6 \text{ cm/s}$ and $\Delta r = 10 \text{ cm}$, the convective growth exponent is $\gamma_0 \Delta r / V_g \approx 3$. Similarly, for $\omega_0/\omega_{CD} = 5.5$, $\omega_2/\omega_{CD} = 4.5$, $\omega_1/\omega_{CD} = 1$, $\zeta_e \approx 0.7$, $V_g \approx 4 \times 10^6 \text{ cm/s}$, and $E_{0x} \approx E_{0y} \approx 200 \text{ V/cm}$, $\gamma_0 \approx 1.5 \times 10^6 \text{ s}^{-1}$, and hence $\gamma_0 \Delta r / V_g \approx 4$. Similar results are obtained for $\omega_0/\omega_{CH} \approx 2.5$.

Another way to optimize growth is to consider decay waves propagating mostly in the y (poloidal) direction, driven by the radial electric field component E_{0x} . In that case, the effective growth distance is approximately $\Delta y \approx 40 \text{ cm}$ whereas $E_{0\perp} \approx E_{0x} \approx 200 \text{ V/cm}$, so that $\gamma_0 \Delta r / V_g \approx 2$, indicating the possibility of a more effective total convective growth.

In any case, these predictions are in reasonable agreement with experimental observations showing a mild growth of ion cyclotron quasimodes and sidebands occurring in a pure hydrogen plasma. Furthermore, the predicted threshold electric fields agree with the electric field calculations for the present experimental conditions.

(b) Decay into an electron QM and an IBW

The low frequency electron QM is characterized by $\omega_1 \ll \omega_{ej}$, $\zeta_e < 1$. In particular, for ASDEX parameters, $\zeta_e \simeq 0.2$, and the growth rate is given by

$$\frac{\gamma_{0j}}{\omega_2} \simeq -\frac{\gamma_{2j}}{\omega_2} + \frac{|\bar{k}_\perp \times \bar{V}_{0\perp}|^2}{8\omega_0^2} \left(\frac{T_e}{T_i} \right) \frac{(1 - \Gamma_0)^2 \sqrt{\pi} \zeta_e}{\left[1 + \frac{T_e}{T_i} (1 - \Gamma_0) \right]^2 P_j} \quad [3]$$

For $T_e/T_i \simeq 1$, $b_i \simeq 9$, $\zeta_e \simeq 0.2$, $\omega_0/\omega_{CH} \simeq \omega_2/\omega_{CH} \simeq 2.4$, we find

$$\gamma_0 + \gamma_2 = 3.5 \times 10^5 \left(\frac{E_\perp (V/cm)}{300} \right)^2 \left(\frac{20}{T_i (eV)} \right) \quad [4]$$

For $E_{0x} \simeq E_{0y} \simeq 200 V/cm$, $T_i \simeq 20 eV$, Eq(4) gives $\gamma_0 \simeq 3 \times 10^5 s^{-1}$. Hence, $\gamma_0 > \gamma_2 \simeq 1 \times 10^5 s^{-1}$ and for $V_g = 4 \times 10^5 cm/s$, $\gamma_0 \Delta r / V_g \simeq 5$ for $\Delta r \simeq 10 cm$. Thus the convective threshold is clearly exceeded.

4. Discussion.

There is clear experimental evidence for the existence of parametric decay phenomena during hydrogen second harmonic heating on ASDEX in both single- and two-ion-species plasmas for a variety of experimental conditions (H-plasma, D/H-plasma with different compositions, with and without NI, various values of magnetic field and plasma current ...) The theoretical predictions are found to be in reasonable agreement with the experimental observations.

Ion Bernstein waves and quasimodes are excited through parametric processes by the high RF electric fields near the fast wave antennas. The question is whether the energy transferred from the pump wave to the short wavelength decay waves can cause significant anomalous absorption. Edge electron heating could be associated with electron Landau damping of the quasimode. Can the ion cyclotron quasimodes cause anomalous ion heating and production of a suprathermal population [4,24]? Edge ion heating could also be a result of ion Bernstein waves, which propagate in the inhomogeneous magnetic field towards an exact ion harmonic (possibly also of impurities), and may be absorbed there by harmonic cyclotron damping.

The parametric decay processes, as well as the occurrence of harmonics of the generator frequency, in some cases also accompanied by parametric decay, may also partly explain why not all the RF power coupled to the plasma is deposited in the central bulk plasma.

According to theoretical predictions, heating regimes at lower fast wave frequencies ($\omega < 2\omega_{CH}$) are less susceptible to parametric instabilities for the electric fields and plasma parameters of interest.

Acknowledgements

This work was carried out at the Institut für Plasmaphysik, Garching, Federal Republic of Germany, in the framework of the EURATOM Mobility of Personnel Scheme. One of the authors, M. Porkolab, was a guest during the summer of 1987; his work was supported by the US Department of Energy under contract DE-ACO2-78ET51013, in the framework of the DOE-ASDEX / ASDEX-UPGRADE collaboration. The authors gratefully acknowledge the excellent support of the ASDEX- and ICRH-teams. R. Van Nieuwenhove and G. Van Oost wish to acknowledge valuable discussions with Professor P. Vandenplas.

References

1. Colestock, P.L., Cohen, S.A., Hosea, J.C., Hwang, D.Q., Green, G.J., et al., J. Vac. Sci. Technol. A3(3) (1985) 1211.
2. Tamai, H., Odajima, K., Matsumoto, H., Ogana, T., Kimura, H., et al., Nucl. Fusion 26(1986) 365.
3. Janeschitz, G., Fussman, G., Noterdaeme, J.-M., Steinmetz, K., Izvozchikov, A., Ryter, F., et al., in Europhysics Conference Abstracts (Proc. 13th Eur. Conf. on Contr. Fus. and Pl. Heat.), Vol. 10 C, I, 407 (1986).
4. Schweer, B., Bay, H.L., Bieger, W., Bogen, P., Hartwig, H., Hintz, E., Höthker, K., Lie, Y.T., Pospieszczyk, A., Ross, G., Rusbüldt, D., Samm, U., Van Nieuwenhove, R., Van Oost, G., in Europhysics Conference Abstracts (Proc. 13th Eur. Conf. on Contr. Fus. and Pl. Heat.), Vol. 10 C, I, 399 (1986).
5. Manning, H.L., Terry, J.L., Lipschultz, B., La Bombard, B., Blackwell, B.D., et al., Nucl. Fusion 26(1986) 1665.
6. Adam, J., Plasma Physics and Controlled Fusion, Vol. 29 (1987) 443.
7. Noterdaeme, J.-M., Janeschitz, G., McCormic, K., Neuhauser, J., Roth, J., Ryter, F., Taglauer, E., Tsois, M., et al., in Europhysics Conference Abstracts (Proc. 14th Eur. Conf. on Contr. Fus. and Pl. Heat.), Vol. 11 D, III, 678 (1987).
8. Samm, U., Bay, H.L., Bogen, P., Hartwig, H., Hintz, E., Höthker, K., Lie, Y.T., Pospieszczyk, A., Ross, G., Rusbüldt, D., Schweer, B., Plasma Physics and Controlled Fusion, Vol. 29 (1987) 1321.
9. Bures, M., Bhatnagar, V.P., Evrard, M.P., Gondhalekar, A., Jacquinet, J., Jones, T.T.C., Morgan, P.D., Start, D.F.H., in Europhysics Conference Abstracts (Proc. 14th Eur. Conf. on Contr. Fus. and Pl. Heat.), Vol. 11D, II, 722 (1987).

10. Steinmetz,K., Fussmann,G., Gruber,D., Niedermeyer,H., Müller,E.R., et al., Plasma Physics and Controlled Fusion, Vol. 28 (1986) 235.
11. Steinmetz,K., Söldner,F.X., Eckhardt,D., Janeschitz,G., Leuterer,F., et al., in Plasma Physics and Controlled Nuclear Fusion Research (Proc. 11th Int. Conf. Kyoto, 1986), Vol.1, IAEA, Vienna (1987) 461.
12. Steinmetz,K., Wesner,F., Niedermeyer,H., Becker,G., Braun,F., et al., J. Vac. Sci. Technol. A4(3) (1986) 1088.
13. Van Nieuwenhove,R., Koch,R., Van Oost,G., Gernhardt,J., Noterdaeme, J.-M., in Europhysics Conference Abstracts (Proc. 14th Eur. Conf. on Contr. Fus. and Pl. Heat.) Vol. 11 D, III, 928 (1987).
14. Skiff,F.N., Wong,K.L., Ono,M., Phys. Fluids 27 (1984) 2205.
15. Messiaen,A.M., Vandenplas,P.E., Peter,G., Electronics Letters 4 (1986) No 2.
16. Brambilla,M., in Europhysics Conference Abstracts (Proc. 14th Eur. Conf. on Contr. Fus. and Pl. Heat.), Vol. 11 D, III, 1011 (1987); also Nucl. Fusion (1988) to be published.
17. Itoh,S.-I., Itoh,K., Fukuyama,A., Morishita,T., Steinmetz,K., Noterdaeme,J.-M, Report MPI Garching IPP III/115, August 1987.
18. Porkolab,M., to be published.
19. Porkolab,M., Phys. Fluids 17 (1974) 1432; also 20 (1977) 2058.
20. Ono,M., Porkolab,M., Chang,R.P.H., Phys. Lett 67A (1978) 379.
21. Ono,M., Porkolab,M., Chang,R.P.H., Phys.Fluids 13 (1980) 1656.
22. Ono,M., Porkolab,M., Chang,R.P.H., Phys. Rev. Lett. 38 (1977) 962.
23. Skiff,F.N., Ono,M., Wong,K.L., Phys. Fluids 27 (1984) 1051.

24. Noterdaeme, J.-M., Ryter, F., Söll, M., Bäumler, J., Becker, G., et. al., in Europhysics Conference Abstracts (Proc. 13th Eur. Conf. on Contr. Fus. and Pl. Heat.), Vol. 10C, II, 137 (1986).

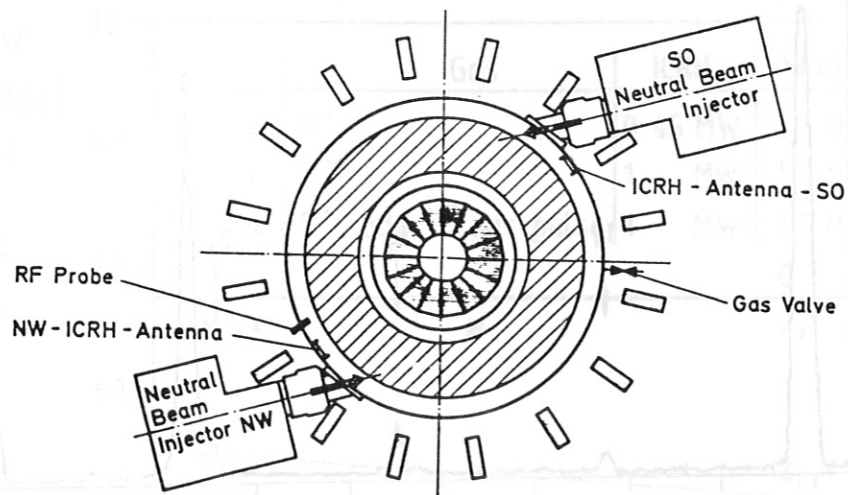


Fig.1(a) Horizontal cross section of ASDEX, showing the relative positions of antennas, neutral injectors, and RF probe.

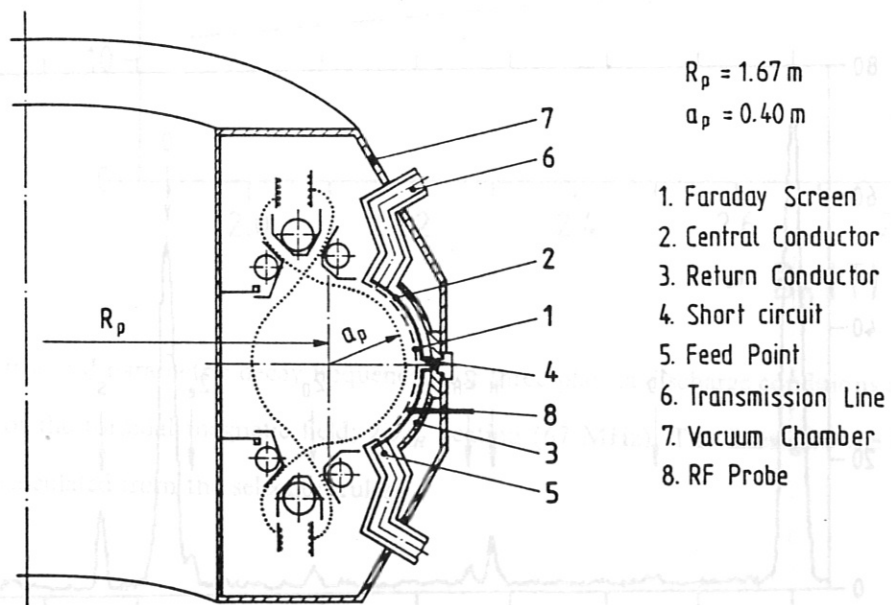


Fig.1(b) Poloidal cross section of ASDEX. The antenna limiter is at $R = 212$ cm and the RF probe tip at $R = 216$ cm.

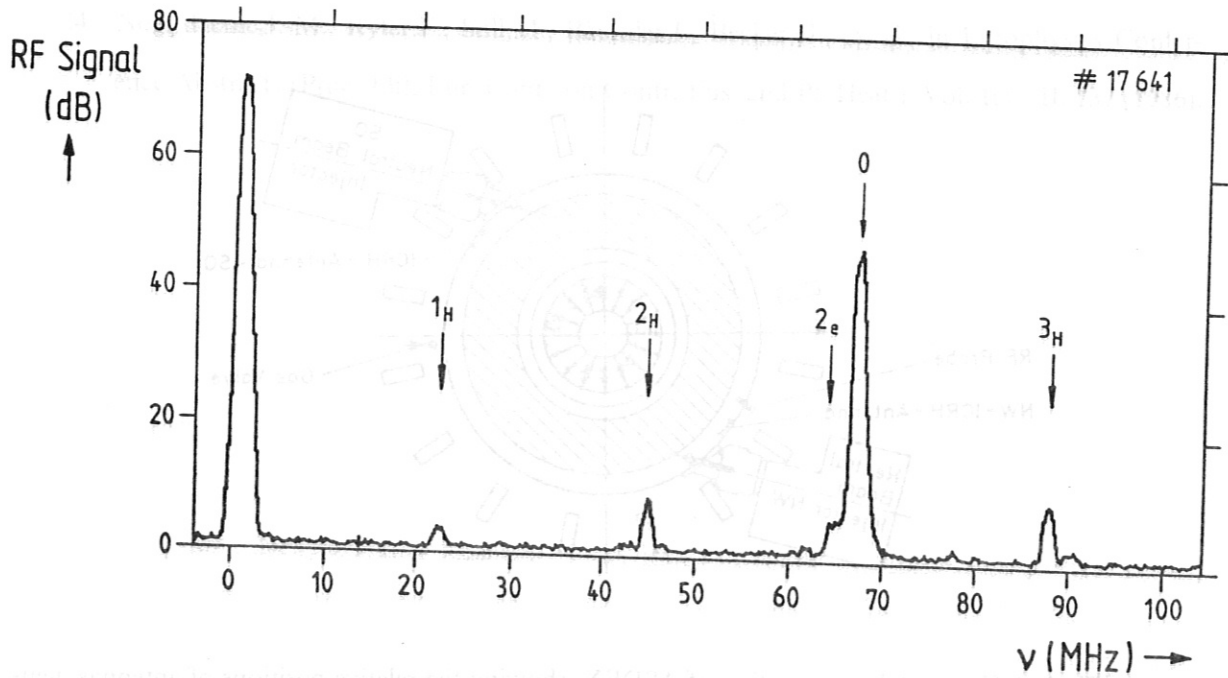


Fig.2(a) Parametric decay spectrum in a mixture of hydrogen (25 %) and deuterium (75 %) with $2\omega_{CH}$ heating (67 MHz, 1 MW); The second harmonic hydrogen cyclotron layer was located at $r = -23$ cm with respect to the plasma centre, for $B_0 = 1.92$ T. Note carefully that the low frequency peak 1_e is not observable due to the zero frequency peak of the spectrum analyzer.

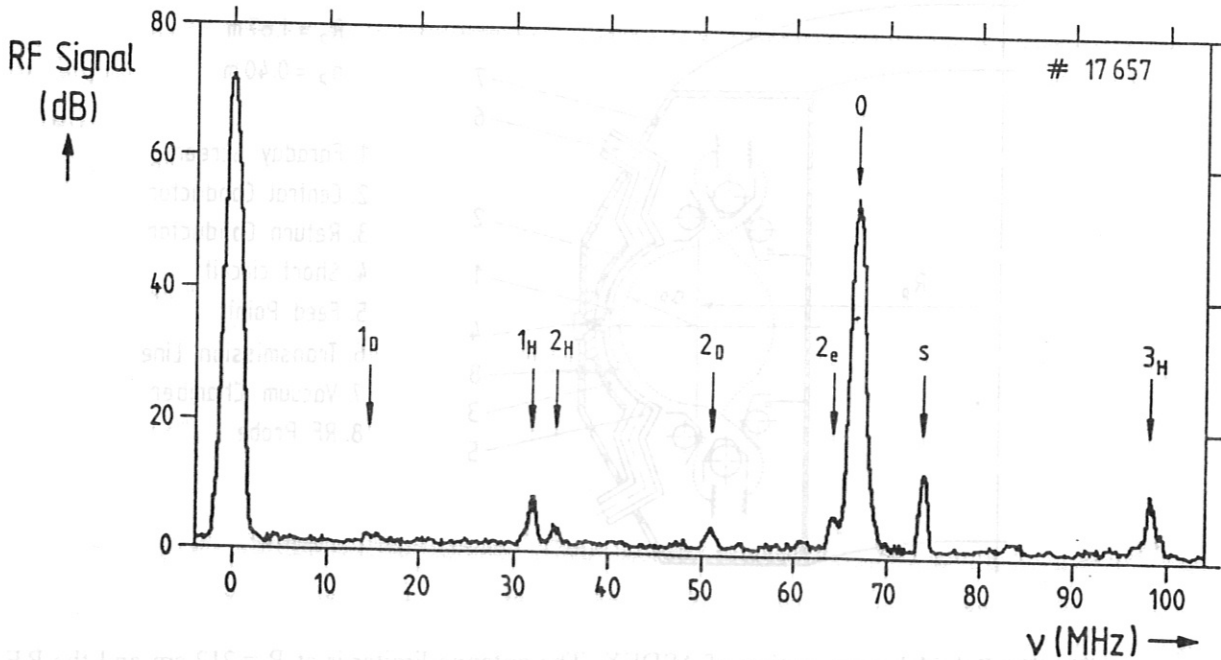


Fig.2(b) Parametric decay spectrum in a mixture of hydrogen (25 %) and deuterium (75 %) with $2\omega_{CH}$ heating (67 MHz, 1 MW). The peak s is due to the second antenna at 74 MHz. The second harmonic hydrogen cyclotron layer was located at $r = 38$ cm with respect to the plasma centre, for $B_0 = 2.73$ T.

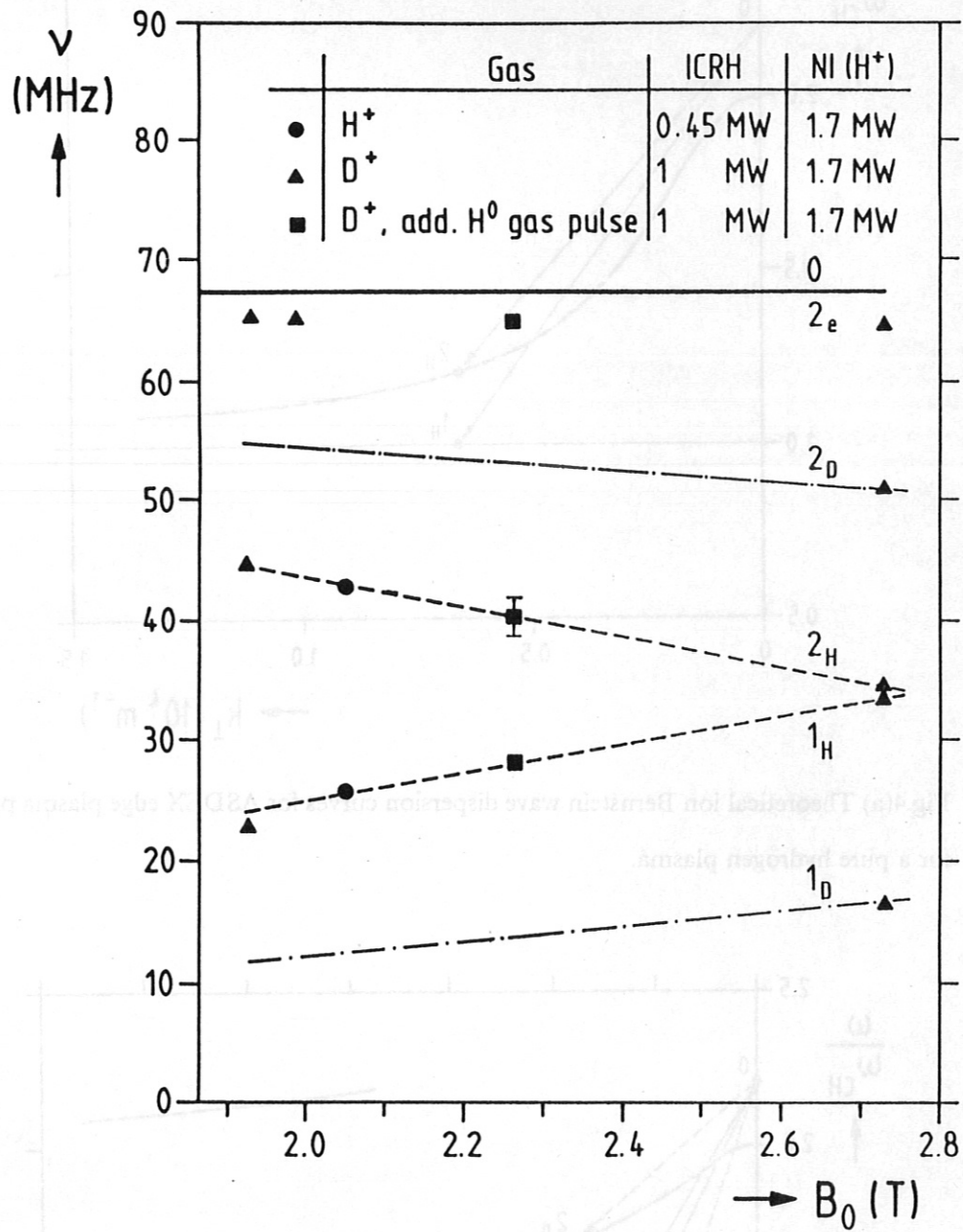


Fig.3 Observed parametric decay frequencies for three plasma discharge conditions and several values of the toroidal magnetic field; $2\omega_{CH}$ heating (67 MHz). The lines give the theoretical values calculated from the selection rules.

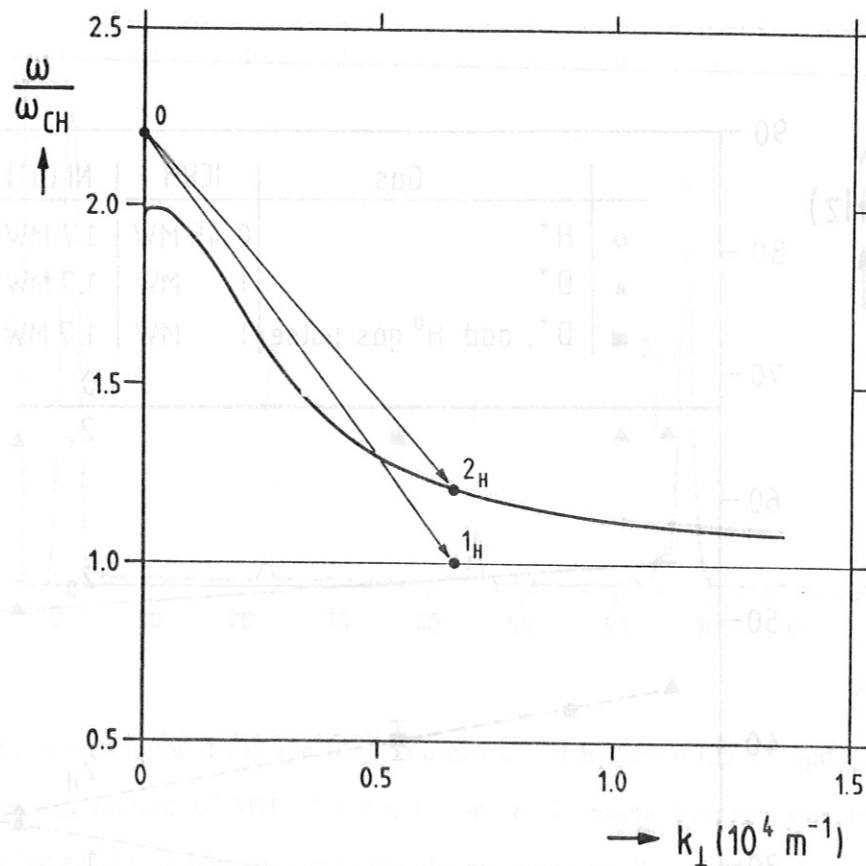


Fig.4(a) Theoretical ion Bernstein wave dispersion curves for ASDEX edge plasma parameters, for a pure hydrogen plasma.

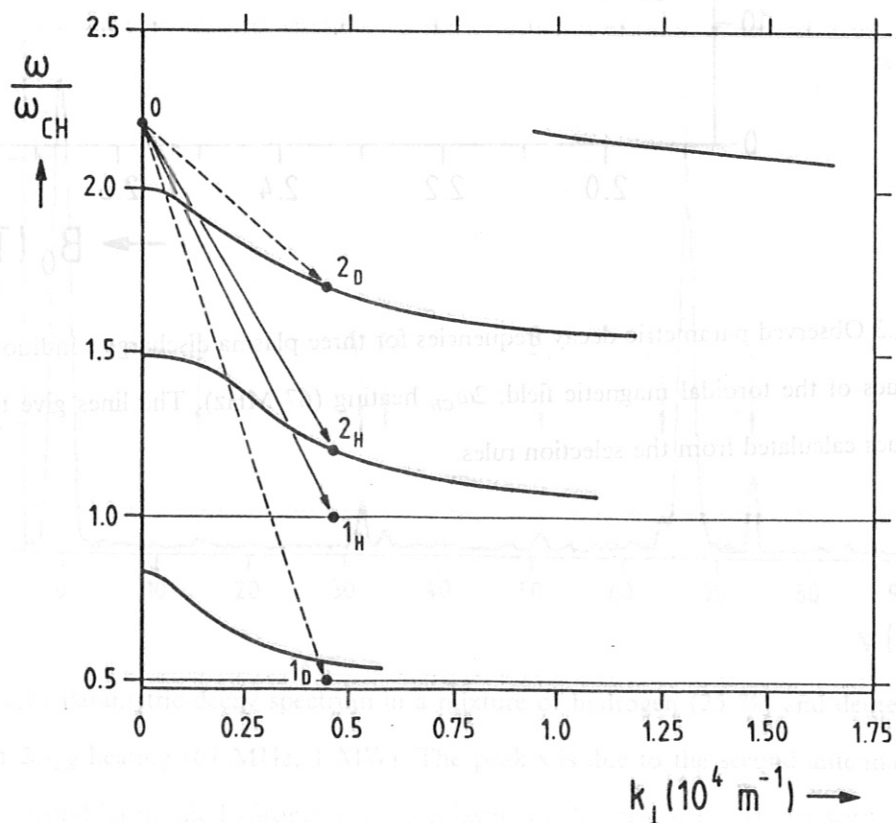


Fig.4(b) Theoretical ion Bernstein wave dispersion curves for ASDEX edge plasma parameters, for a mixture of hydrogen (25 %) and deuterium (75 %).